Carrier Aggregation for Cooperative Cognitive Radio Networks

Panagiotis D. Diamantoulakis, *Student Member, IEEE*, Koralia N. Pappi, *Member, IEEE*, Sami Muhaidat, *Senior Member, IEEE*, George K. Karagiannidis, *Fellow, IEEE*, and Tamer Khattab, *Member, IEEE*

***Abstract*—The ever-increasing demand for mobile Internet and high-data-rate applications poses unique challenging requirements for 5G mobile networks, including spectrum limitations and massive connectivity. Cognitive radio and carrier aggregation (CA) have recently been proposed as promising technologies to overcome these challenges. In this paper, we investigate joint relay selection and optimal power allocation in an underlay cooperative cognitive radio with CA, taking into account the availability of multiple carrier components in two frequency bands, subject to outage probability requirements for primary users (PUs). The secondary user network employs relay selection, where the relay that maximizes the end-to-end sum rate is selected, assuming both decode-and-forward and amplify-and-forward relaying. The resulting optimization problems are optimally solved using convex optimization tools, i.e., dual decomposition and an efficient iterative method, allowing their application in practical implementations. Simulation results illustrate that the proposed configuration exploits the available degrees of freedom efficiently to maximize the SU rate, while meeting the PU average outage probability constraints.**

***Index Terms*—Amplify-and-forward (AF), carrier aggregation (CA), cognitive radio (CR), decode-and-forward (DF), dynamic power allocation, interference, relay selection.**

I. Introduction

COGNITIVE radio (CR) is an intelligent radio technology that can adapt its transmission parameters according to the environment. CRs have shown to be very efficient in maximizing spectrum utilization due to their inherent spectrum sensing capability. A CR network consists of primary users (PUs), i.e., users with higher priority utilizing a particular band in the spectrum, and secondary users (SUs), i.e., users wishing to opportunistically access that spectrum, provided that they guarantee the PUs' quality of service (QoS) [1]–[3]. Research on CR has focused on three spectrum sharing paradigms, namely, underlay, overlay, and interweave [1]. In this paper, we focus on underlay cognitive networks [3], [4], in which a cooperative SU transmits, while maintaining the interference imposed on the PUs under a specific threshold.

The available spectrum for the SU transmission is commonly dispersed [5], since the spectral usage of an SU may extend among different or heterogeneous networks [6]. Therefore, a secondary CR user may transmit and receive over multiple dispersed bands. In order to facilitate transmission over dispersed spectrum, discontiguous (or noncontiguous) orthogonal frequency division multiplexing (D-OFDM or NC-OFDM) was first proposed and investigated in [7]–[10], which assume the employment of existing OFDM technology at the transceivers. However, this technique cannot be applied in spectrum segments with substantially different characteristics.

Therefore, another technology that allows the usage of multiple spectrum segments is carrier aggregation (CA). It has been included in the 3GPP LTE-Advanced (LTE-A) telecommunication system architecture [11], [12], where it allows the aggregation of a maximum of 100 MHz of bandwidth, leading to wireless access, which achieves higher data rates, and improving the energy efficiency. It can aggregate component carriers (CCs), which belong to either the same band (intraband CA) or different carrier bands (interband). Interband CA is naturally noncontiguous, which means that the aggregated subbands are noncontiguous as well; however, intraband CA can be either contiguous or noncontiguous. In the case of continuous CA, two or more CCs can be aggregated within the same band, utilizing the same baseband architecture. On the contrary, in the case of noncontinuous CA, CCs can be aggregated using separate baseband radio frequency chains [13].

A. Motivation

1) Cooperative CR Networks: In the context of CR, the performance of cooperative networks in which SUs can act as relays has been extensively investigated. For example, relay-assisted communication using D-OFDM is investigated in [14] and [15], aiming at the improvement of either the diversity or the throughput of the secondary links. Furthermore, various works on

Manuscript received May 27, 2016; revised October 2, 2016; accepted November 7, 2016. Date of publication December 2, 2016; date of current version July 14, 2017. The work of P. D. Diamantoulakis, G. K. Karagiannidis, and T. Khattab was supported by the NPRP under Grant NPRP 6-1326-2-532 from the Qatar National Research Fund (a member of Qatar Foundation). This work was presented in part at the IEEE Wireless Communications and Networking Conference (WCNC), Doha, Qatar, Apr. 2016. The review of this paper was coordinated by Prof. D. B. da Costa.

P. D. Diamantoulakis and G. K. Karagiannidis are with the Department of Electrical and Computer Engineering, Aristotle University of Thessaloniki, 54124 Thessaloniki, Greece (e-mail: padiaman@auth.gr; geokarag@auth.gr).

K. N. Pappi is with the Department of Electrical and Computer Engineering, Aristotle University of Thessaloniki, 54124 Thessaloniki, Greece, and also with Intracom S. A. Telecom Solutions, 57001 Thessaloniki, Greece (e-mail: kpappi@auth.gr).

S. Muhaidat is with the Khalifa University, 127788 Abu Dhabi, United Arab Emirates, and also with the Centre for Communication Systems Research, University of Surrey, Surrey GU2 7XH, U.K. (e-mail: muhaidat@ieee.org).

T. Khattab is with the Electrical Engineering, Qatar University, 2713 Doha, Qatar (e-mail: tkhattab@ieee.org).

Color versions of one or more of the figures in this paper are available online at http://ieeexplore.ieee.org.

Digital Object Identifier 10.1109/TVT.2016.2635112

cooperative CR networks focus on the power allocation between the weak direct link and the dual-hop link, and on the relay selection among multiple available relaying nodes. Optimal power allocation in an underlay single-carrier cooperative network with two receivers is investigated in [16], where the PU imposes constraints on the instantaneous received interference. Resource allocation for a multiuser secondary cooperative network with maximal ratio combining (MRC) is optimized in [17]. In [18], power allocation for a cooperative transmission in a secondary network employing MRC is optimized in terms of symbol error probability. In [19], power allocation of a secondary network performing MRC is optimized in a decentralized manner, targeting specific signal-to-noise ratio (SNR) for the SU. Furthermore, best relay selection has been investigated in CR networks with the aim to optimize the outage probability or the bit error rate of the secondary underlay network in [20]–[24].

2) Cooperative CR Networks With CA: In CA systems, the combined spectrum presents diverse propagation characteristics. As a result, the combination of CA and CR networks has been mainly investigated for heterogeneous networks and small cells, e.g., the coordination of multiple SUs was investigated in [25], traffic balancing in [26], and resource and data scheduling in [27]. On the other hand, in cooperative CA systems, communication in aggregated high-frequency bands experiences high attenuation and path loss. In such cases, relays are used not only for diversity [28], [29], but also for coverage extension [30], [31]. Thus, different data streams can be sent via the direct link and the dual-hop link, over multiple carriers.

However, the combination of both cooperative communications and CA with CR networks has not been thoroughly investigated, since there have been only sporadic results on joint relay selection and dynamic power allocation in multicarrier underlay cognitive networks. In [32], the authors aim at maximizing the total throughput, when only two data streams are sent over orthogonal frequencies by the SU, through a direct and a dual-hop Amplify-and-Forward (AF) link. However, the provided solution cannot be directly extended to the case of multiple CCs due to the need of power allocation at the relay. A similar system model and optimization scheme with multiple CCs is examined in [33] and [34], where again AF relaying is considered. However, the authors resort to oversimplified suboptimal solutions based on equivalent noise minimization over each link. Moreover, the interference imposed by the PU is considered to be perfectly known and canceled at the SU, which increases the complexity of the decoding process and creates implementation difficulties. It is worth noting that most of the assumptions made in [33] and [34] do not match the principles of underlay cognitive networks and CA. Additionally, the aforementioned works assume perfect channel state information (CSI) for the links between PU-SU, which is not realistic to acquire in practice, while the case of decode-and-forward (DF) relaying is not investigated.

B. Contribution

Unlike recent literature, in this paper, we investigate the application of CA in an underlay CR network, which also utilizes multiple relays, employing relay selection. We focus on interband CA, where the characteristics of the aggregated bands can be very different. In general, the higher frequency band creates smaller coverage radius, compared to the lower frequency band that produces larger coverage radius, since the path loss increases proportionally to frequency and distance. Motivated by this, we assume that the high-frequency band cannot be directly used by the SU to transmit information with acceptable quality, which is resolved by the utilization of the relays. Consequently, in order to fully exploit the available bandwidth in both bands, a cooperative SU is considered, which transmits over multiple CCs, both in the direct and the dual-hop link, with the aim to increase its achievable rate without causing harmful interference to the PUs. The assumed system model allows the SU pair to communicate efficiently over multiple bands, while the available relays contribute not only to throughput maximization but also to coverage extension for the high-frequency carriers, where direct transmission is not feasible.

In order to boost SU performance and minimize interference at the PUs, we formulate a joint power allocation and relay selection optimization problem, appropriate for throughput efficient communication in relay-assisted CA systems. In particular, the contribution of this paper can be summarized as follows.

1) An optimization problem is formulated for each of the AF and DF relaying protocols, which performs power allocation among the CCs of two frequency bands. The low-frequency band is used for communication of the SU pair via the direct link and the high-frequency band is used for communication via the dual-hop link. Moreover, the formulated optimization also performs relay selection for the dual-hop link, based on the overall maximization of the throughput, under specific constraints for the outage probability of each PU pair.
2) The constraints that are set by each of the PUs, regard their average outage probability and not the instantaneous interference they receive from the SU network. As such, these constraints require less frequent feedback from the PUs, since they depend on long-term metrics. In order to further reduce PU feedback, a minimum feedback scheme toward the SU network is considered, based on quantization of the applicable SU transmit power thresholds. Thus, the proposed communication and optimization scheme is a suitable candidate for practical underlay CR networks, because it does not require extensive or frequent signaling from the PUs, minimizing the feedback as much as possible.
3) The formulated power allocation problems are optimally solved. For this purpose, convex optimization tools and dual decomposition are applied. Furthermore, the optimal values are calculated using a simple, efficient, and fast-converging iterative algorithm. To the best of the authors knowledge, a similar optimization problem has not been considered in the literature for the DF case.

Extensive simulation results illustrate the performance gains for the SU, when CA is applied in cognitive networks, without degrading the QoS that the PUs enjoy. The simulation scenarios also examine the tradeoff between the number of PU feedback quantization bits and the throughput gains, proving that only a few bits are actually needed. Finally, results regarding the power

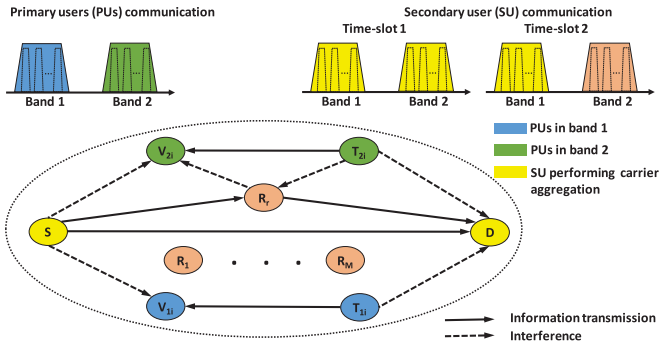

Fig. 1. Synopsis of PUs communication, SU transmission, and received interference.

allocation and relay usage highlight the importance of selection of the best-situated relay.

C. Organization

The rest of this paper is organized as follows. Section II demonstrates the system and channel model, and elucidates the technologies used, i.e., CA, CR, and AF/DF relaying. Section III includes the PU requirements, where the instantaneous interference threshold, which is usually assumed, is now replaced by an average outage probability threshold. Section IV defines the achievable rate for the SU, regarding both relaying protocols. In Section V, the power allocation problem is introduced, while it is solved in Sections VI and VII, for the cases of DF and AF relaying protocol, respectively. In Section VIII, the simulations and the derived results are analyzed. Finally, Section IX concludes this paper.

II. System Model

In this paper, an underlay SU network is considered, consisting of a source (S) and a destination (D), which employs CA, aggregating CCs from two different frequency bands, indexed by $l = 1, 2$. In order to achieve higher rates, the SU aggregates a number of N_l CCs from the lth band. The lower frequency band is denoted by $l = 1$, while the higher frequency band is denoted by $l = 2$. Based on the long-term statistics and the distances between the available nodes, the high-frequency band is considered to be used over the two-hop link for coverage, while the low-frequency band is used only through the direct link, to minimize the complexity and cost of the relays, which are equipped with the RF chains of the high-frequency band only. One licensed PU, consisting of a transmitter $T_{l,i}$ and a receiver $V_{l,i}$, operates over the ith CC of the lth band $\forall i, l$. That is, there are $N_1 + N_2$ operating PUs. The system model is depicted in Fig. 1, where one PU operating over each frequency band is depicted on the network sketch for simplicity.

Each PU sets a maximum probability of outage threshold, which prevents the SU from transmitting with high power over each CC. The SU utilizes the direct link between S and D for the N_1 CCs of the lower frequency band. Over the higher frequency band ($l = 2$), due to high path loss, we assume that there is no line-of-sight, thus the SU utilizes a half-duplex relay, selected out of M available relays, which are denoted by R_r, $r = 1, 2, \ldots, M$. Communication between S and D is divided into two time slots. In the first time slot, S transmits over both frequency bands, and all relays receive over the high-frequency band, while D receives over the low-frequency band. In the second time slot, S transmits only over the low-frequency band, while the selected relay transmits over the high-frequency band, and D receives through all bands. The communication during both time slots is also illustrated in Fig. 1.

The goals of the analysis that follows are: 1) the optimal power allocation both at the source and the relay and 2) the optimal relay selection based on the total achievable rate. Depending on the selected relay, a different optimal power allocation can be computed, while the best relay selection is based on the overall maximization of the achievable rate of the SU.

All nodes are equipped with a single antenna and the codebooks of all nodes are considered to be long zero mean and unit variance complex Gaussian. Each channel coefficient between any two nodes, e.g., J and Q, follows a complex Gaussian distribution, i.e., $h_{jq|l,i} \sim \mathcal{CN}(0, 1/L_{jq|l,i})$, where $l = 1, 2$ and $i = 1, 2, \ldots, N_l$. The additive noise at any node Q follows a complex Gaussian distribution with $n_{q|l,i} \sim \mathcal{CN}(0, W_{l,i}N_0)$, with $W_{l,i}$ being the bandwidth of the ith CC of the lth band and N_0 being the noise power spectral density. The notation used throughout this paper is summarized in Table I.

III. PUs Communication

Each $T_{l,i}$ transmits a codeword $z_{l,i}$ toward the corresponding $V_{l,i}$ over the ith CC in the lth band. The received signal at each $V_{l,i}$ is given by

$$y_{v|l,i} = \sqrt{P_{t|l,i}} h_{tv|l,i} z_{l,i} + I_{\mathrm{SU}|l,i} + n_{v|l,i} \tag{1}$$

where $I_{\mathrm{SU}|l,i}$ is the interference imposed by the SU.

The power allocation scheme of the SU must take the interference thresholds set by the PUs and their desired QoS into account. To this end, we first present the types of thresholds that can be set by the PUs and the feedback that is needed to be sent to the SU.

A. PU Instantaneous Interference Threshold

In underlay cognitive networks, the SU network operation is designed so that the amount of interference imposed on the PUs is acceptable. A good measure for the aforementioned is the outage probability of the PUs. Particularly, the outage probability of each PU is confined by a threshold $\bar{P}_{\mathrm{out}}$ such that, in the worst-case scenario, recovering data at each V_l is possible. One solution is constricting the instantaneous interference, imposed by the SU on each PU, under a corresponding threshold. According to the instantaneous channels between the S and the PUs and the corresponding threshold, specific power limits for the secondary source and relay transmission are imposed. For each CC in the first band and for the first time slot of each CC in the second band, it is $I_{\mathrm{SU}|l,i} = \sqrt{P_{s|l,i}} h_{sv|l,i} x_{l,i}$, and thus, for

TABLE I
NOTATION

Variable	Explanation	Variable	Explanation
M	Number of available relays	$x_{l,i}$	SU information symbol
$l=1,2$	Frequency band index	$z_{l,i}$	PU information symbol
N_l	Number of CCs in the lth band	$n_{q\|l,i}$	AWGN noise at node Q
$(\cdot)_{l,i}$	Value for the lth band and ith CC	$y_{q\|l,i}$	Received symbol at node Q
S	SU source node	$\hat{x}_{2,i}$	Reencoded SU information symbol (DF)
D	SU destination node	N_0	AWGN power spectral density
$T_{l,i}$	PU transmitter	$I_{\mathrm{SU}\|l,i}$	Interference imposed by SU on PU
$V_{l,i}$	PU receiver	$P^{[I_{l,i}]}$	Instantaneous interference power threshold set by a PU
R_r	The r^{th} relay	$K_{q\|l,i}$	Power threshold for node Q, set by a PU
$P_{q\|l,i}$	Power transmitted by node Q	$\gamma_{l,i}$	End-to-end SINR
$h_{jq\|l,i}$	Channel coefficient of path $J\rightarrow Q$	$\gamma_{jq\|l,i}$	SINR of path $J\rightarrow Q$
$L_{jq\|l,i}$	Path loss of path $J\rightarrow Q$	$\mathcal{P}_q$	Power vector of node Q
$G_{r\|l,i}$	Amplification factor of relay R_r (AF)	$\mathcal{R}_{l\|r}$	Rate of lth band selecting the relay R_r
$(\cdot)^{\mathrm{AF}}$	Value for AF relaying	$P_{\mathrm{out}(S)\|l,i}$	Outage probability of a PU caused by S
$(\cdot)^{\mathrm{DF}}$	Value for DF relaying	$P_{\mathrm{out}(R_r)\|l,i}$	Outage probability of a PU caused by R_r
$W_{l,i}$	CC bandwidth	$P^{\mathrm{IF}}_{\mathrm{out}\|l,i}$	Interference-free outage probability of a PU

the power of the interfering signal, it must hold that

$$P_{s|l,i} \leq \frac{P^{[I_{l,i}]}}{|h_{sv|l,i}|^2}. \tag{2}$$

Similarly, the transmitted power of each R_r in the second time slot for the second band must satisfy [3], [35]

$$P_{r|2,i} \leq \frac{P^{[I_{2,i}]}}{|h_{rv|2,i}|^2} \tag{3}$$

where $P^{[I_{l,i}]}$ are the corresponding instantaneous interference power thresholds.

In practice, in order for the SU to optimally perform power allocation, the secondary network should be aware of $h_{rv|2,i}$ and $h_{sv|l,i}$ $\forall l \in \{1,2\}$ and $\forall i$. Obtaining all these channel coefficients either requires transmission of training symbols from each $V_{l,i}$, and then, performing channel estimation at S and at each R_r, or estimating them at each $V_{l,i}$ and feeding back the channel estimates to S and each R_r, respectively. In both cases, a large overhead due to training symbols and/or feedback is transmitted, which reduces the bandwidth efficiency of the system and makes the synchronization of PU-SU costly.

B. PU Average Outage Probability

To reduce overhead, we propose a more flexible constraint on the average outage probability of the PUs and not on the instantaneous interference. Thus, the PU feeds the acceptable power limits for S and each R_r back to the SU, based on the statistics of the channels. From (1), in the first band and for the first time slot in the second band, the interference imposed by SU on each PU is $I_{\mathrm{SU}|l,i} = I_{S\rightarrow V_{l,i}}$. Therefore, the PU signal-to-interference-plus-noise ratio (SINR) is given by $\gamma_{\mathrm{PU}(S)|l,i} = \frac{P_{t|l,i}|h_{tv|l,i}|^2}{P_{s|l,i}|h_{sv|l,i}|^2+W_{l,i}N_0}$. Similarly to [36, Appendix A], if $R_{0|l,i}$ is the desired data rate and $\bar{R}_{0|l,i} = 2^{\frac{R_{0|l,i}}{W_{l,i}}} - 1$, then the outage probability of the PU is given by

$$P_{\mathrm{out}(S)|l,i} = 1 - \frac{L_{sv|l,i}P_{t|l,i}\exp(-L_{tv|l,i}\bar{R}_{0|l,i}W_{l,i}N_0/P_{t|l,i})}{L_{sv|l,i}P_{t|l,i}+L_{tv|l,i}P_{s|l,i}\bar{R}_{0|l,i}}. \tag{4}$$

Accordingly, in the second time slot and the second band, the interference is caused by the selected relay and the corresponding outage probability is

$$P_{\mathrm{out}(R_r)|2,i} = 1 - \frac{L_{rv|2,i}P_{t|2,i}\exp(-L_{tv|2,i}\bar{R}_{0|2,i}W_{2,i}N_0/P_{t|2,i})}{L_{rv|2,i}P_{t|2,i}+L_{tv|2,i}P_{r|2,i}\bar{R}_{0|2,i}}. \tag{5}$$

When there is no interference imposed on each PU, the interference free outage probability of each PU is given by

$$P^{\mathrm{IF}}_{\mathrm{out}|l,i} = 1 - \exp(-L_{tv|l,i}\bar{R}_{0|l,i}W_{l,i}N_0/P_{t|l,i}) \tag{6}$$

which is the best case scenario for the outage performance of each PU. For a specific average outage probability threshold $\bar{P}_{\mathrm{out}|l,i}$ for which it must hold that $\bar{P}_{\mathrm{out}|l,i} > P^{\mathrm{IF}}_{\mathrm{out}|l,i}$, the outage probabilities given in (4) and (5) must always be below this threshold. Using (4) and (5) and solving, the transmitted powers, the corresponding power thresholds for S and each R_r in each frequency band and each CC are calculated as follows:

$$P_{s|l,i} \leq \underbrace{\left\lceil \left(\frac{\exp\left(-\frac{L_{tv|l,i}\bar{R}_{0|l,i}W_{l,i}N_0}{P_{t|l,i}}\right)}{1-\bar{P}_{\mathrm{out}|l,i}} - 1 \right) \frac{L_{sv|l,i}P_{t|l,i}}{L_{tv|l,i}\bar{R}_{0|l,i}} \right\rceil^-}_{K_{s|l,i}} \tag{7}$$

$$P_{r|2,i} \leq \underbrace{\left\lceil \left(\frac{\exp\left(-\frac{L_{tv|2,i}\bar{R}_{0|2,i}W_{2,i}N_0}{P_{t|2,i}}\right)}{1-\bar{P}_{\mathrm{out}|2,i}} - 1 \right) \frac{L_{rv|2,i}P_{t|2,i}}{L_{tv|2,i}\bar{R}_{0|2,i}} \right\rceil^-}_{K_{r|2,i}} \tag{8}$$

where $\lceil . \rceil^-$ means quantization to the closest smaller quantization level. The values $P_{r|2,i}$ and $K_{r|2,i}$ apply only for $l=2$, since there is a dual-hop link only over the high-frequency band. Assuming that each PU can send feedback of only a number of $\log_2(\mathcal{K})$ bits, the distinct values of the corresponding power threshold are $\mathcal{K}$. The selected power level at which the SU or the relay should use is transmitted toward their corresponding node at the beginning of each time slot right after channel estimation. By using this technique at each time slot, the PU needs

to send only $\log_2(\mathcal{K})$ bits of information via a feedback link, reducing the required feedback link bandwidth. These transmissions could be performed via feedback links operating in another narrow frequency band.

IV. SU Communication

A. SU Direct Link Over the First Band

During the first time slot, the power of the source S of the SU is divided between the two frequency bands. During the second time slot, the transmitted power is reallocated only over the direct link. Please note that in each band and during each time slot, S sends different noninterfering messages, since we do not seek to increase diversity, but to increase data rate, which is the main motivation for using CA. Moreover, the channel coefficients are considered constant over two consecutive time slots. The transmission from $T_{l,i}$ is causing interference in the ith CC. Thus, in the first time slot, the received signal at D is given by

$$y_{d|1,i} = \sqrt{P_{s|1,i}}h_{sd|1,i}x_{1,i} + \sqrt{P_{t|1,i}}h_{td|1,i}z_{1,i} + n_{d|1,i} \quad (9)$$

where $x_{1,i}$ is the transmitted symbol. The received SINR at D over the ith CC is then given by

$$\gamma_{1,i} = \frac{P_{s|1,i}|h_{sd|1,i}|^2}{P_{t|1,i}|h_{td|1,i}|^2 + W_{1,i}N_0}. \quad (10)$$

If $P'_{s|l,i}$ is the reallocated power during the second time slot instead of $P_{s|l,i}$, the corresponding SINR is denoted by $\gamma'_{1,i}$ hereafter.

B. SU Relay-Assisted Link Over the Second Band

In the first time slot, S transmits data symbols over each CC of the second band toward the relays. Furthermore, transmission from each $T_{2,i}$ is causing interference during both time slots. Thus, the received signal at the rth relay node over the ith CC is

$$y_{r|2,i} = \sqrt{P_{s|2,i}}h_{sr|2,i}x_{2,i} + \sqrt{P_{t|2,i}}h_{tr|2,i}z_{2,i} + n_{r|2,i}. \quad (11)$$

When two or more CCs are aggregated in the second frequency band, the power and information allocation over the CCs depends on the relaying protocol. When the AF protocol is applied, then the relay forwards a scaled version of its received signal to D over the same CC. That is, the relay cannot divide the received information over the CCs anew. However, when the DF protocol is applied, the source information can be redivided over the available CCs. According to the aforementioned, we discern our analysis depending on the relaying protocol below.

1) AF Relaying: With AF relaying, in the second time slot, the rth relay—if selected—normalizes its received signal over the ith CC by

$$G_{r|2,i} = \left(\frac{P_{r|2,i}}{P_{s|2,i}|h_{sr|2,i}|^2 + P_{t|2,i}|h_{tr|2,i}|^2 + W_{2,i}N_0}\right)^{\frac{1}{2}} \quad (12)$$

and then, it forwards the scaled version to D, assuming that all required power and channel values are known, as it will be further explained in Section IV-D. The received signal at D is then given by

$$y^{\mathrm{AF}}_{d|2,i} = G_{r|2,i}h_{rd|2,i}y_{r|2,i} + \sqrt{P_{t|2,i}}h_{td|2,i}z_{2,i} + n_{d|2,i} \quad (13)$$

and thus, the received end-to-end instantaneous SINR at D over the ith CC of the second frequency band is then given by

$$\gamma^{\mathrm{AF}}_{2,i} = \frac{\gamma_{sr|2,i}\gamma_{rd|2,i}}{\gamma_{sr|2,i} + \gamma_{rd|2,i} + 1} \quad (14)$$

where

$$\gamma_{sr|2,i} = \frac{P_{s|2,i}|h_{sr|2,i}|^2}{P_{t|2,i}|h_{tr|2,i}|^2 + W_{2,i}N_0} \quad (15)$$

$$\gamma_{rd|2,i} = \frac{P_{r|2,i}|h_{rd|2,i}|^2}{P_{t|2,i}|h_{td|2,i}|^2 + W_{2,i}N_0}. \quad (16)$$

2) DF Relaying: With DF relaying protocol, the relay first denoises the received signal and decodes the received information. Then, it reencodes and forwards the decoded information towards the destination through the N_2 available CCs over the second band. In the first time slot, the received signal at the rth relay is given by (11), and thus, the SINR of the first hop of the rth relay is given by (15).

The relay reencodes the decoded information in multiple streams and transmits one symbol over each CC, denoted by $\hat{x}_{2,i}$, with average power $P_{r|2,i}$. Thus, the received signal at the destination is

$$y^{\mathrm{DF}}_{d|2,i} = \sqrt{P_{r|2,i}}h_{rd|2,i}\hat{x}_{2,i} + \sqrt{P_{t|2,i}}h_{td|2,i}z_{2,i} + n_{d|2,i}. \quad (17)$$

Accordingly, the SINR of the second hop is given by (16).

C. Total Achievable Rate

Based on the Shannon capacity formula, we consider that the achievable transmission rate of the SU when a relay R_r is selected, during the first time slot and over the first frequency band can be written as

$$\mathcal{R}_{1|r} = \sum_{i=1}^{N_1} W_{1,i}\log_2\left(1 + \gamma_{1,i}\right) \quad (18)$$

while for the second time slot, it is denoted by

$$\mathcal{R}'_{1|r} = \sum_{i=1}^{N_1} W_{1,i}\log_2\left(1 + \gamma'_{1,i}\right). \quad (19)$$

Similarly, the achievable rate over the second band during both time slots for AF relaying is given by

$$\mathcal{R}^{\mathrm{AF}}_{2|r} = \sum_{i=1}^{N_2} \frac{1}{2}W_{2,i}\log_2\left(1 + \gamma^{\mathrm{AF}}_{2,i}\right) \quad (20)$$

while for DF relaying is given by

$$\mathcal{R}^{\mathrm{DF}}_{2|r} = \min\left(\sum_{i=1}^{N_2} \frac{1}{2}W_{2,i}\log_2(1 + \gamma_{sr|2,i}), \sum_{i=1}^{N_2} \frac{1}{2}W_{2,i}\log_2(1 + \gamma_{rd|2,i})\right). \quad (21)$$

TABLE II
COMMUNICATION OF THE SU NETWORK

Band	Time-Slot 1	Time-Slot 2
$l=1$	Nodes: $S \to D$ Power: $P_{s\|1,i}$ over the ith CC Rate: $\mathcal{R}_{1\|r^*}$	Nodes: $S \to D$ Power: $P'_{s\|1,i}$ over the ith CC Rate: $\mathcal{R}'_{1\|r^*}$
$l=2$	Nodes: $S \to R_r^*$ Power: $P_{s\|2,i}$ over the ith CC	Nodes: $R_r^* \to D$ Power: $P_{r\|2,i}$ over the ith CC
	Rate: $\mathcal{R}_{2\|r^*}^{\mathrm{AF/DF}}$	

In the aforementioned expressions, $\frac{1}{2}$ appears due to the half-duplex operation of the relay. For the DF protocol, since the information is redivided over the CCs at the relay, the rate is constrained by the minimum of the sum of the capacities, achieved over each hop. The total achievable rate during two time slots is given by

$$\mathcal{R}_{\mathrm{tot}|r} = \left(\frac{1}{2}\mathcal{R}_{1|r} + \frac{1}{2}\mathcal{R}'_{1|r}\right) + \mathcal{R}_{2|r}^{\mathrm{AF/DF}}. \tag{22}$$

The communication of the SU is summarized in Table II, where r^* is the best (selected) relay.

D. CSI

For the proposed optimization, nodes R_r and D require full CSI of the secondary network. Furthermore, they require CSI of the corresponding paths from the primary transmitters $T_{l,i}$, which is acquired from pilot symbols send by the PUs. The primary receivers, $V_{l,i}$, only need knowledge of the path loss values $L_{sv|l,i}$ and $L_{rv|2,i}$. The PUs send minimum feedback to the SU (a number of $\log_2 \mathcal{K}$ bits indicating the corresponding power thresholds, as they were defined in Section III), which is updated only when the $L_{sv|l,i}$ and $L_{rv|2,i}$ values change. Finally, the selected relay sends the optimal power allocation to S via feedback link. The channel estimation and required feedback are summarized in Algorithm 1.

Algorithm 1: Channel Estimation and Feedback.

1: **Low-frequency band (l=1):**
2: Nodes S and $T_{1,i}$ transmit orthogonal pilot symbols (2 pilot symbols over each CC).
3: Node D estimates the channel coefficients $h_{sd|1,i}$ and $h_{td|1,i}$ for each CC. Every V_{1i} estimates the channel coefficient $h_{tv|1,i}$ and the path loss $L_{sv|1,i}$.
4: **High-frequency band (l=2):**
5: Nodes S and $T_{2,i}$ transmit orthogonal pilot symbols (two pilot symbols over each CC).
6: All nodes R_r estimate the channel coefficients $h_{sr|2,i}$ and $h_{tr|2,i}$ for each CC. Node D estimates the channel coefficients $h_{td|2,i}$ for each CC. Every V_{2i} estimates the channel coefficient $h_{tv|2,i}$ and the path loss $L_{sv|2,i}$.
7: All nodes R_r transmit orthogonal pilot symbols (M pilot symbols over each CC).
8: Node D estimates the channel coefficients $h_{rd|2,i}$ for each CC. Every $V_{2,i}$ estimates the path loss $L_{rv|2,i}$.
9: **After estimation:**
10: D sends its estimated channel values to all relays.
11: If $L_{sv|l,i}$ and $L_{rv|2,i}$ have changed, the PUs update and resend their power thresholds to the SU.
12: **After optimization:**
13: The selected relay sends its computed power allocation to S.

V. OPTIMAL POWER ALLOCATION AND RELAY SELECTION

A. Problem Formulation

In the following, we describe the optimization performed by each relay. The optimal power allocation of S and R_r—if selected—can be written as

$$\begin{aligned}
\max_{\mathcal{P}_s,\mathcal{P}'_s,\mathcal{P}_r} \quad & \mathcal{R}_{\mathrm{tot}|r} \\
\text{s.t.} \quad & \mathrm{C}_1: 0 \le P_{s|l,i} \le K_{s|l,i} \\
& \mathrm{C}_2: 0 \le P'_{s|l,i} \le K_{s|l,i} \\
& \mathrm{C}_3: 0 \le P_{r|l,i} \le K_{r|l,i} \\
& \mathrm{C}_4: \sum_{l=1}^{2}\sum_{i=1}^{N_l} P_{s|l,i} \le P_{s,\max}
\end{aligned}$$

$$\begin{aligned}
& \mathrm{C}_5: \sum_{i=1}^{N_1} P'_{s|1,i} \le P_{s,\max} \\
& \mathrm{C}_6: \sum_{i=1}^{N_2} P_{r|2,i} \le P_{r,\max}
\end{aligned} \tag{23}$$

where $\mathcal{P}_s = \{P_{s|l,i} : l \in \{1,2\}, i \in \{1,2,\ldots,N_l\}\}$, $\mathcal{P}'_s = \{P'_{s|1,i} : i \in \{1,2,\ldots,N_1\}\}$, and $\mathcal{P}_r = \{P_{r|2,i} : i \in \{1,2,\ldots,N_2\}\}$ are the source power allocation vectors for the first and second time slot and the relay power allocation vector, respectively. This optimization is performed with the aim to find the maximum achievable rate $\mathcal{R}_{\mathrm{tot}|r}$ that the rth relay can achieve. In the aforementioned, $P_{s,\max}$ and $P_{r,\max}$ are the maximum values for the power that can be transmitted by S and R_r, respectively, and they are imposed by regulations or hardware specifications.

B. Problem Separation and Relay Selection

Problem (23) can be completely separated in two disjoint problems, since the reallocated power over the low-frequency band ($\mathcal{P}'_s$) for the second time slot is independent of the relay selection and power allocation during the first time slot. Thus, the two separate problems can be written as

Problem 1

$$\begin{aligned}
\max_{\mathcal{P}_s,\mathcal{P}_r} \quad & \frac{1}{2}R_{1|r} + R_{2|r}^{AF/DF} \\
\mathbf{s.t.} \quad & \mathrm{C}_1, \mathrm{C}_3, \mathrm{C}_4, \mathrm{C}_6
\end{aligned} \tag{24}$$

Problem 2

$$\max_{\mathcal{P}_s'} \quad \frac{1}{2} R'_{1|r}$$
$$\mathbf{s.t.} \quad \mathrm{C}_2, \mathrm{C}_5. \tag{25}$$

Relay selection cannot be determined solely by the channel realizations, but it is heavily based on 1) the power allocation and 2) the position of the relay with respect to the PUs, which defines the power thresholds. Thus, the selection must be based on the actual achievable rate, which requires the power allocation solution. However, for each relay, the optimal power allocation, which can maximize its rate does not depend on the rest of the relays; its location and its channel coefficients are the only parameters, which are required. To this end, the optimal power allocation of the source is calculated for each relay, for the case that this specific relay might be selected, before the actual relay selection. Afterwards, the relay, which achieves the highest total rate $\mathcal{R}_{\mathrm{tot}|r}$ is selected. Since the optimization of the transmission $S \rightarrow D$ during the second time-slot (Problem 2) yields the same results for all relays, each relay solves solely Problem 1. Then, the selection is reduced to

$$R_r^* = \arg\max_r \mathcal{R}_{\mathrm{tot}|r} = \arg\max_r \left(\frac{1}{2} \mathcal{R}_{1|r} + \mathcal{R}_{2|r} \right) \tag{26}$$

while Problem 2 is solved after the relay selection and *only* by the selected relay. Finally, the selected relay sends the optimal power allocation as feedback to S.

VI. Solution for the Case of DF Relaying

A. Problem 1: $N_2 \geq 2$

When the relays employ DF relaying, the achievable rate is given by the minimum of the total achievable rate of each of the dual hop, which, however, is not a purely analytic expression. To this end, the optimization problem (Problem 1) is transformed into its epigraph form [30], [37]. The auxiliary variable R is used in order to describe the limitation that the one hop imposes to the other. Therefore, the optimization problem (Problem 1) for the case of DF can now be written as

$$\max_{\mathcal{P}_s, \mathcal{P}_r} \quad \sum_{i=1}^{N_1} \frac{1}{2} W_{1,i} \log_2(1 + \gamma_{1,i}) + R$$
$$\mathbf{s.t.} \quad \mathrm{C}_1, \mathrm{C}_3, \mathrm{C}_4, \mathrm{C}_6$$
$$\mathrm{C7}: \sum_{i=1}^{N_2} \frac{1}{2} W_{2,i} \log_2(1 + \gamma_{sr|2,i}) \geq R$$
$$\mathrm{C8}: \sum_{i=1}^{N_2} \frac{1}{2} W_{2,i} \log_2(1 + \gamma_{rd|2,i}) \geq R. \tag{27}$$

The extra constraints C7 and C8 represent the hypograph of the original optimization problem, i.e., Problem 1.

Remark 1: The transformed optimization problem in (27) is jointly concave with respect to the optimization variables, since the Hessian matrix of its objective function is negative semidefinite and the inequality constraints are all convex. Moreover, it satisfies Slater's constraint qualification, and thus, it can now be optimally and efficiently solved with dual decomposition, since the duality gap between the dual and the primal solution is zero. More importantly, it is guaranteed that its global optimum solution can now be obtained in polynomial time [37]. Please note that the same conclusions hold for any other optimization problem of similar structure that follows the aforementioned conditions.

By using dual decomposition, the optimization problem in (27) can be iteratively solved in two consecutive layers, namely *Layer 1* and *Layer 2*, which are explained later. In each iteration, one subproblem for each CC in thefirst band and two identical subproblems for each CC in the second band are solved in parallel in Layer 1 by using the Karush–Kuhn–Tucker (KKT) conditions for a fixed set of Lagrange multipliers (LMs). The LMs are then updated in Layer 2 using the gradient method.

Layer 1: In this layer, the optimal power allocation is calculated, by using the following theorem.

Theorem 1: The optimal values of $P_{s|1,i}^*$, $P_{s|2,i}^*$, and $P_{r|2,i}^*$ are given by

$$P_{s|1,i}^* = \left[\frac{W_{1,i}}{2\lambda_1 \ln(2)} - \frac{\Gamma_{1|1,i}}{|h_{sd|1,i}|^2} \right]_0^{K_{s|1,i}} \tag{28}$$

where $[\cdot]_x^y = \min(\max(x, \cdot), y)$, while

$$P_{s|2,i}^* = \left[\frac{\lambda_3 W_{2,i}}{2\lambda_1 \ln(2)} - \frac{\Gamma_{1|2,i}}{2|h_{sr|2,i}|^2} \right]_0^{K_{s|2,i}} \tag{29}$$

$$P_{r|2,i}^* = \left[\frac{W_{2,i}(1-\lambda_3)}{2\lambda_2 \ln(2)} - \frac{\Gamma_{2|2,i}}{|h_{rd|2,i}|^2} \right]_0^{K_{r|2,i}} \tag{30}$$

where

$$\Gamma_{1|l,i} = |h_{tr|2,i}|^2 P_{t|2,i} + N_0 W_{2,i} \tag{31}$$

$$\Gamma_{2|2,i} = |h_{td|2,i}|^2 P_{t|2,i} + N_0 W_{2,i}. \tag{32}$$

Proof: The proof of Theorem 1 is given in Appendix A.

The power allocation in (28)–(30) can be interpreted as a multilevel water-filling scheme, in which the water levels of different CCs can be different. Please note that the water levels $\frac{W_{1,i}}{2\lambda_1 \ln(2)}$, $\frac{W_{2,i}(1-\lambda_3)}{2\lambda_2 \ln(2)}$, and $\frac{W_{2,i}(1-\lambda_3)}{2\lambda_2 \ln(2)}$, are generally higher for CCs with more available bandwidth. Interestingly, taking into account the second terms of (28)–(30), it is observed that a larger value of $\Gamma_{j|l,i}\ \forall j \in \{1,2\}$ results to a lower value of allocated power, in order to reduce the impact of the received interference by the PUs.

Layer 2: Since the dual function is differentiable, the gradient method can be used to update the LMs as follows:

$$\lambda_1(t+1) = \left[\lambda_1(t) - \zeta_1(t) \left(P_{s,\max} - \sum_{l=1}^{2} \sum_{i=1}^{N_l} P_{s|l,i} \right) \right]^+ \tag{33}$$

$$\lambda_2(t+1) = \left[\lambda_2(t) - \zeta_2(t) \left(P_{r,\max} - \sum_{i=1}^{N_2} P_{r|l,i} \right) \right]^+ \tag{34}$$

where $[\cdot] = \max(0, \cdot)$, $t \geq 0$ is the iteration index, and $\zeta_i(t)$ are positive step sizes, chosen in order to satisfy the infinite travel

condition [38]. Also, as it can be observed by (54), for the LM λ_3 it must hold that $0 \leq \lambda_3 \leq 1$, and in each iteration it is given by

$$\lambda_3(t+1) = \left[\lambda_3(t) - \zeta_3(t)\left(\sum_{i=1}^{N_2}\frac{1}{2}W_{2,i}\log_2(1+\gamma_{sr|2,i}) - \sum_{i=1}^{N_2}\frac{1}{2}W_{2,i}\log_2(1+\gamma_{rd|2,i})\right)\right]_0^1. \quad (35)$$

Remark 2: When the optimization problem satisfies the conditions described in Remark 1, it is guaranteed that the iteration between the two layers converges to the optimal solution of the *primal problem*, if the chosen step sizes satisfy the infinite travel condition [37], [38]

$$\sum_{t=1}^{\infty}\zeta_i(t) = \infty \forall\, i. \quad (36)$$

B. Problem 1: The Special Case When $N_2 = 1$

With DF relaying and assuming that $N_2 = 1$, there is no more need to transform the initial problem (Problem 1) to its epigraph form, as in (27). Instead, the optimization Problem 1 can now be simplified, considering the observation that γ_2^{DF} is the minimum of the SINR values of the two hops. Thus, if the dual-hop link of a CC of the second band is limited by the second hop, there is no benefit from increasing the SINR of the first hop, by increasing $P_{s|2,i}$. Therefore, by considering the constraint $\gamma_{sr|2,i} \leq \gamma_{rd|2,i}$, we set $\tilde{K}_{s|1,i} = K_{s|1,i}$ and

$$\tilde{K}_{s|2,1} = \min\left(\frac{P_{r|2,1}|h_{rd|2,1}|^2(P_{t|2,1}|h_{tr|2,1}|^2 + W_{2,1}N_0)}{|h_{sr|2,1}|^2(P_{t|2,1}|h_{td|2,1}|^2 + W_{2,1}N_0)}K_{s|2,1}\right) \quad (37)$$

and thus, Problem 1 for the case of DF can now be written as

$$\begin{aligned}\max_{\mathcal{P}_s} \quad & \frac{1}{2}R_{1|r} + R_{2|r}^{\mathrm{DF}} \\ \mathbf{s.t.} \quad & \tilde{\mathrm{C}}1: \ 0 \leq P_{s|l,i} \leq \tilde{K}_{s|l,i} \\ & \forall l \in \{1,2\},\ \forall i \in \{1,2,\ldots,N_l\} \\ & \mathrm{C}_4. \end{aligned} \quad (38)$$

Considering Remark (1), we next iteratively solve the optimization problem in (38) using dual decomposition. By doing so, in Layer 1, the subproblems of the power allocation of the source are solved for the corresponding fixed set of LMs, which are updated in Layer 2. Please note that only one subproblem is now solved for the second band in each iteration.

Theorem 2: The optimal power allocation of carrier i for the first band is given by (28), while for the second band is given by

$$\hat{P}_{s|2,1}^* = \left[\frac{|h_{sr|2,1}|^2 W_{2,1} - 2\lambda_1 \ln(2)\Gamma_{1|2,1}}{2\lambda_1|h_{sr|2,1}|^2\ln(2)}\right]_0^{\tilde{K}_{s|2,1}}. \quad (39)$$

Note that the LM λ_1 is updated by (33).

Proof: The proof of Theorem 2 is given in Appendix B.

C. Discussion for Problem 2

The analysis in order to find the optimal solution for Problem 2 is similar to that of (38), ignoring the term $R_{2|r}^{\mathrm{DF}}$, respectively. So, in Layer 1, $P_{s|1,i}^* = \left[\hat{P}_{s|1,i}\right]_0^{K_{s|1,i}}$, with $\hat{P}'_{s|1,i}$ given by (28), while in Layer 2, the LM λ_1 is updated according to (33).

The solution for Problem 2 can also be applied for a special case of Problem 1, i.e., $N_2 = 0$. Problem 1 is the simplified to

$$\begin{aligned}\max_{\mathcal{P}_s} \quad & \frac{1}{2}\mathcal{R}_{1|r} \\ \mathbf{s.t.} \quad & \mathrm{C}_1, \mathrm{C}_4. \end{aligned} \quad (40)$$

Thus, it can be solved exactly as the optimization problem 2, replacing $P'_S, \mathrm{C}_2,$ and C_5 with $P_S, \mathrm{C}_1,$ and C_4, respectively.

VII. Solution for the Case of AF Relaying

In this section, the solution of the optimization problem in (24), i.e., Problem 1, is solved for the case of AF relaying protocol. Please note that the solution of Problem 2 is omitted, because it is not affected by the utilized relaying protocol.

A. Problem 1: $N_2 \geq 2$

When $N_2 \geq 2$, problem 1 is nonconvex, and thus, it cannot be solved with acceptable complexity. Therefore, in order to transform it into a convex problem, we consider the following well-known tight approximation for the end-to-end SINR of the rth relay, especially in the medium and high SINR region, as shown in [39]

$$\gamma_{2,i}^{\mathrm{AF}} \approx \tilde{\gamma}_{2i}^{\mathrm{AF}} = \frac{\gamma_{sr|2,i}\gamma_{rd|2,i}}{\gamma_{sr|2,i} + \gamma_{rd|2,i}}. \quad (41)$$

Problem 1 can now be written as

$$\begin{aligned}\max_{\mathcal{P}_s,\mathcal{P}_r} \quad & \frac{1}{2}\mathcal{R}_{1|r} + \tilde{\mathcal{R}}_{2|r}^{\mathrm{AF}} \\ \mathbf{s.t.} \quad & \mathrm{C}_1, \mathrm{C}_3, \mathrm{C}_4, \mathrm{C}_6 \end{aligned} \quad (42)$$

where

$$\tilde{R}_{2|r}^{\mathrm{AF}} = \sum_{i=1}^{N_2}\frac{1}{2}W_{2,i}\log_2(1+\tilde{\gamma}_{2i}^{\mathrm{AF}}). \quad (43)$$

Considering Remark 1, we can solve the optimization problem in (42) iteratively, using dual decomposition. In each iteration in Layer 1, one subproblem for each CC in the first band and two identical subproblems for each CC in the second band are solved in parallel for a fixed set of LMs, which are then updated in Layer 2.

Layer 1: In this layer, the optimal power allocation is calculated, by using the following theorem.

Theorem 3: The optimal solutions $P^*_{s|1,i}$, $P_{s|2,i}$, and $P^*_{r|2,i}$ are given by (28) as

$$\hat{P}^*_{s|2,i} = \Bigg[-\frac{\Gamma_{1|2,i}}{|h_{sr|2,i}|^2} + \frac{1}{\ln(4)} \times \left(\frac{|h_{rd|2,i}|^2 W_{2,i} \Gamma_{1|2,i}}{|h_{rd|2,i}|^2 \lambda_1 \Gamma_{1|2,i} - |h_{sr|2,i}|^2 \lambda_2 \Gamma_{2|2,i}} + \sqrt{\Gamma_{3|2,i}} \right) \Bigg]_0^{K_{s|2,i}} \tag{44}$$

and

$$\hat{P}^*_{r|2,i} = \left[\sqrt{\frac{\Gamma_{4|2,i}}{4\ln(2)}} - \frac{|h_{sr|2,i}|^2 \hat{P}_{s|2,i} \Gamma_{2|2,i} (|h_{sr|2,i}|^2 \hat{P}_{s|2,i} + 2\Gamma_{1|2,i})}{2|h_{rd|2,i}|^2 \Gamma_{1|2,i} (|h_{sr|2,i}|^2 \hat{P}_{s|2,i} + \Gamma_{1|2,i})} \right]_0^{K_{r|2,i}} \tag{45}$$

respectively. In the aforementioned solutions, $\Gamma_{1|2,i}$ and $\Gamma_{2|2,i}$ are given by (31) and (32), respectively, while $\Gamma_{3|2,i}$ and $\Gamma_{4|2,i}$ are given in (46) and (47), shown at the bottom of this page, respectively.

Proof: The proof of Theorem 3 is given in Appendix C.

Layer 2: Since the dual function is differentiable, the gradient method can be used to update the LMs λ_1 and λ_2, which are given by (33) and (34), respectively. Taking into account Remark 2, it is proved that the iteration between the two layers converges to the optimal solution.

B. Problem 1: Special Case when $N_2 = 1$

When $N_2 = 1$, the relay transmits with its maximum power, i.e., $P_{r|2,1} = \max(K_{s|2,1}, P_{r,\max})$ if $P_{s|2,1} \geq 0$. Thus, the optimization problem of power allocation of S and the selected relay can be simplified to

$$\begin{aligned} \max_{\mathcal{P}_s} \quad & \frac{1}{2}\mathcal{R}_{1|r} + \mathcal{R}^{\mathrm{AF}}_{2|r} \\ \mathbf{s.t.} \quad & \mathrm{C}_1, \mathrm{C}_4. \end{aligned} \tag{49}$$

Layer 1: The optimal power allocation values can be calculated by considering the following theorem.

Theorem 4: The optimal power allocation values $P^*_{s|1,i}$ and $P^*_{s|2,1}$ are given by (28) and

$$\hat{P}_{s|2,1} = \left[\left(-\frac{|h_{rd|2,1}|^2 P_{r|2,1} \Gamma_{1|2,1} \left(|h_{rd|2,1}|^2 P_{r|2,1} + 2\Gamma_{2|2,1} \right)}{2|h_{sr|2,1}|^2 \Gamma_{2|2,1} \left(|h_{rd|2,1}|^2 P_{r|2,1} + \Gamma_{2|2,1} \right)} + \sqrt{\frac{\Gamma_{5|2,1}}{4\ln(2)}} \right) \right]_0^{K_{s|2,1}} \tag{50}$$

where $\Gamma_{5|2,1}$ is given by (48), shown at the bottom of this page.

Proof: The proof of Theorem 4 is given in Appendix D. ■

Layer 2: Applying the gradient method, the LM λ_1 is given by (33).

VIII. Simulation Results

In this section, we present numerical and simulation results for an SU network, which aggregates one or two CCs in each band. The coordinates of the SU nodes are $S(-5, 0)$, $D(5, 0)$, while the M available relays are situated on the x-axis, equally spaced between points $(-4, 0)$ and $(4, 0)$. The coordinates of the PU nodes are $T_{1,1}(-2, 7)$, $V_{1,1}(2, 7)$, $T_{1,2}(-2, 10)$, and $V_{1,2}(2, 10)$ for the low-frequency band and $T_{2,1}(-2, -7)$, $V_{2,1}(2, -7)$, $T_{2,2}(-2, -10)$, and $V_{2,2}(2, -10)$ for the high-frequency band. The path loss between any node pair, e.g., the pair of nodes J and Q, is modeled with the bounded path loss model $L_{jq|l,i} = 1 + d^{\alpha_l}_{jq}$ [40], where d_{jq} is the distance between nodes and α_l is the path loss exponent for each band, which is assumed to be $\alpha_1 = 2$ and $\alpha_2 = 2.5$. All coordinates and distances are measured in meters. We further consider normalized bandwidth $W_{1,i} = W_{2,i} = W = 1$ Hz, while $P_{s,\max} = P_{r,\max}$. It is assumed that the PUs transmit with power ratio $P_{t|l,i}/N_0 = 15$ dB. Finally, for the PUs holds that $P^{\mathrm{IF}}_{\mathrm{out}|l,i} = 10^{-6}$ and $\bar{P}_{\mathrm{out}|l,i} = 1.1 \times 10^{-6}$.

In Fig. 2, the achievable rate of the SU is depicted, when AF (solid lines) or DF (dash-dotted lines) relaying is considered, with respect to different $P_{s,\max}$ values. The results are presented for $M = 2, 4, 6$ available relays, while two cases are assumed, that is, when one CC or two CCs in each band are aggregated. A first observation on the effect of CA on the performance is that the aggregation of more CCs (four instead of two in total) increases the achievable rate, without increasing the total transmitted power. Since the spectrum is shared with the licensed users and the SU transmits without disturbing the PUs, CA offers substantial improvement in performance without the need of

$$\Gamma_{3|2,i} = \frac{\lambda_2 \Gamma_{2|2,i} \Gamma_{1|2,i} \left(|h_{rd|2,i}|^2 |h_{sr|2,i}|^2 W_{2,i} - |h_{sr|2,i}|^2 \lambda_2 \Gamma_{2|2,i} \ln(4) + |h_{rd|2,i}|^2 \lambda_1 \Gamma_{1|2,i} \ln(4) \right)^2}{|h_{rd|2,i}|^2 |h_{sr|2,i}|^2 \lambda_1 \left(|h_{sr|2,i}|^2 \lambda_2 \Gamma_{2|2,i} - |h_{rd|2,i}|^2 \lambda_1 \Gamma_{1|2,i} \right)^2} \tag{46}$$

$$\Gamma_{4|2,i} = \frac{|h_{sr|2,i}|^4 \hat{P}^2_{s|2,i} \Gamma_{2|2,i} \left(2|h_{rd|2,i}|^2 W_{2,i} \Gamma_{1|2,i} (|h_{sr|2,i}|^2 \hat{P}_{s|2,i} + \Gamma_{1|2,i}) + |h_{sr|2,i}|^4 \lambda_2 \hat{P}^2_{s|2,i} \Gamma_{2|2,i} \ln(2) \right)}{|h_{rd|2,i}|^4 \lambda_2 \Gamma^2_{1|2,i} \left(|h_{sr|2,i}|^2 \hat{P}_{s|2,i} + \Gamma_{1|2,i} \right)^2} \tag{47}$$

$$\Gamma_{5|2,1} = \frac{|h_{rd|2,1}|^4 P^2_{r|2,1} \Gamma_{1|2,1} \left(2|h_{sr|2,1}|^2 W_{2,1} \Gamma_{2|2,1} \left(|h_{rd|2,1}|^2 P_{r|2,1} + \Gamma_{2|2,1} \right) + |h_{rd|2,1}|^4 \lambda_1 P^2_{r|2,1} \Gamma_{1|2,1} \ln(2) \right)}{|h_{sr|2,1}|^4 \lambda_1 \Gamma^2_{2|2,1} \left(|h_{rd|2,1}|^2 P_{r|2,1} + \Gamma_{2|2,1} \right)^2} \tag{48}$$

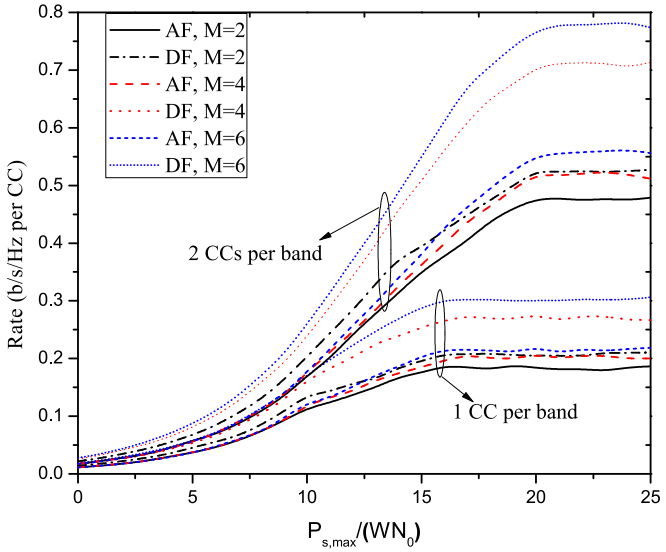

Fig. 2. Achievable rate with AF and DF relaying for $M = 2, 4, 6$ available relays and for different number of CCs.

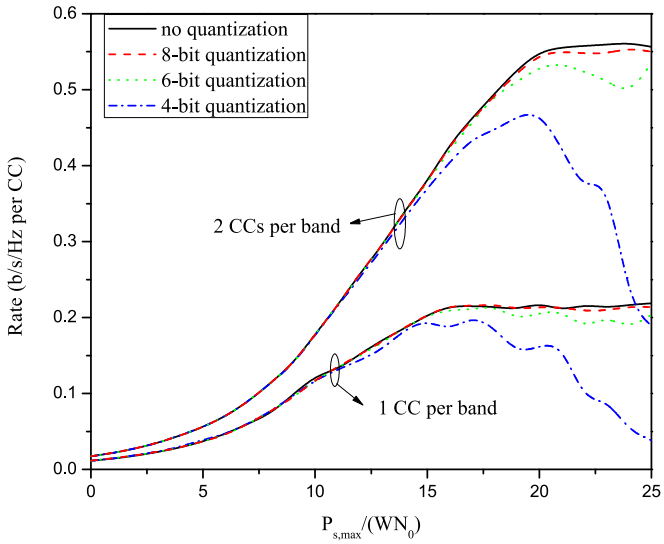

Fig. 3. Achievable rate with AF relaying for 4-,6-, and 8-bit feedback quantization, with $M = 6$ available relays and for different number of CCs.

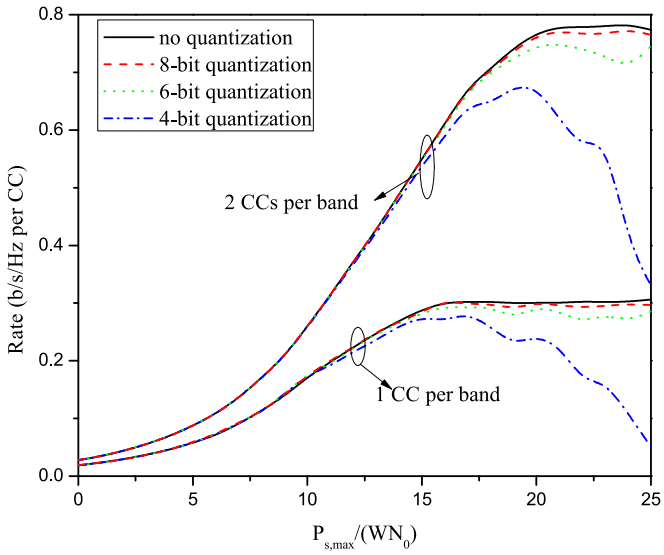

Fig. 4. Achievable rate with DF relaying for 4-, 6-, and 8-bit feedback quantization, with $M = 6$ available relays and for different number of CCs.

increased energy consumption. The performance improvement is expected, since the available spectrum at the SU is double when two CCs in each band are aggregated, however, the rate that is achieved is more than double with respect to the achieved rate when one CC in each band is aggregated.

Another observation from Fig. 2 is that the achievable rate reaches a floor when $P_{s,\max}$ increases, for all cases of aggregated CCs and available relays (M). This is reasonable for high SNR values, since the power transmitted by S is constricted by the thresholds set by the PUs. This means that, although the total available power for transmission at S can be $P_{s,\max}$, the actual total transmitted power may be less, since otherwise it will impose unacceptable interference on the PUs. Another useful observation is that this floor can be substantially improved by adding more available relays for the high-frequency band, thus enhancing the performance of the SU network. The gain from adding more relays is more evident, when the number of aggregated CCs is larger, since the links benefiting from the selection are more.

Moreover, from Fig. 2, it is evident that when DF relaying is considered, the network achieves higher rates compared to the application of AF relaying, for all cases of different number of aggregated CCs and different number of available relays. A notable difference, comparing to the AF case, is that when DF is applied, the performance is substantially improved when more available relays are added. This is an expected result, since, in the case of DF relaying, the information bits received at the relay can be reallocated over the bands, adding to the degrees of freedom of the proposed optimization, and thus, making the selection of the best relay more important.

Figs. 3 and 4 depict the performance of the secondary network, in the case when the PUs send quantized feedback for the transmit power threshold of the secondary nodes, for AF and DF relaying, respectively. The performance of the network when full feedback is available is also depicted for reference. The results include the cases when the feedback is of 4, 6, or 8 bits, which corresponds to $\mathcal{K} = 16, 64, 256$ distinct power levels. We assume that this quantization divides the value range $\{0, P_{s,\max}\}$ in equally spaced distinct power levels. Although DF relaying performs better than AF relaying, in both protocols, the effect of quantization on the PU feedback is similar. More specifically, for a low number of quantization bits, e.g., 4-bit quantization, the performance degrades when the transmit power reaches a floor, in contrast to the case of full feedback where the rate does not decrease, but it also reaches a floor. This can be explained as follows: The value range $[0, P_{s,\max}]$ is divided into equally spaced distinct power levels according to the available quantization bits, however, the actual power transmitted by the SU is lower than $P_{s,\max}$, since the nodes' transmit powers are constricted by the power threshold set by the PU. Thus, the actual power range is smaller, while some power levels are included in the quantization range but they are

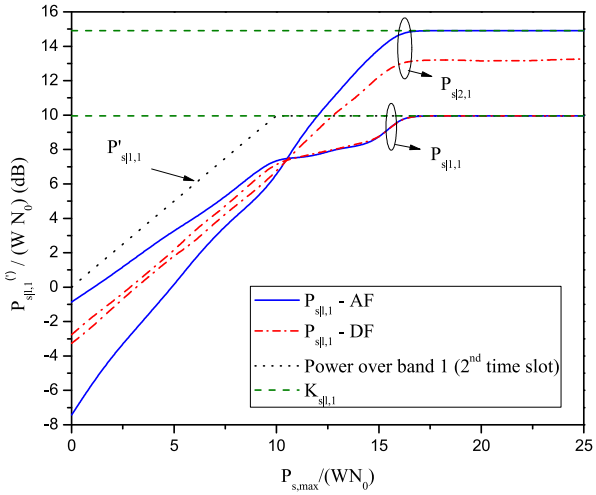

Fig. 5. Power allocation at the source when AF or DF relaying is applied, for $M = 6$ available relays and for one CC per frequency band.

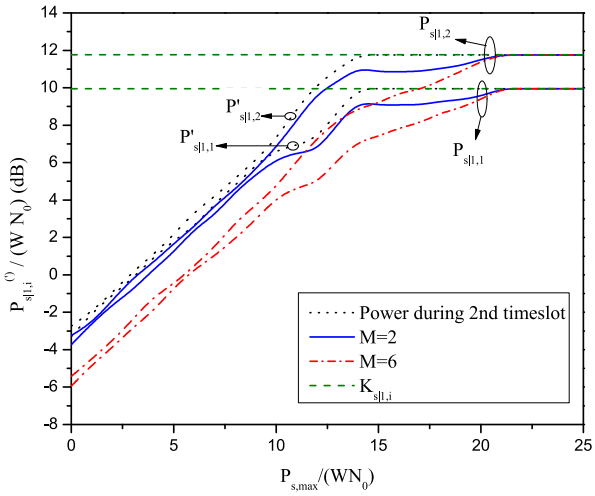

Fig. 6 Power allocation at the source over the low-frequency band, when DF relaying is applied, for $M = 2, 6$ available relays and for two CCs per frequency band.

never used. This problem could be overcome with the adoption of nonequally spaced power levels. On the other hand, a small increase of the number of quantization bits seems to greatly improve the performance, since the quantization resolution of the actual power range is improved. Both figures show that only 8 bits of feedback are enough for the SU network to perform with almost equal rate as in the case that there is full feedback by the PUs. This is a very important conclusion, since it highlights the applicability of the method, while the feedback from the PUs is kept as small as possible.

Fig. 5 compares the power allocation at the source of the SU, when one CC per band is aggregated, for the AF and DF relaying protocols. More specifically, the allocation among the two frequencies (one in each band) for AF relaying is depicted with red solid lines, whereas for DF, it is depicted with blue solid lines. The black dash-dot line represents the power allocation over the carrier of the first band during the second time slot, which is the same both for AF and DF relaying; since S does not transmit over the second band due to the half-duplex operation of the relay, all the available power is allocated over the first band, until it reaches the power threshold for approximately $P_{s,\max}/(WN_0) = 10$ dB. No quantization is assumed, i.e., the PU sends the exact values of the power thresholds as feedback, which are also represented in the figure with dashed green lines. When AF relaying is applied, the power values for both frequencies reach the thresholds set by the PUs. Moreover, for low SNR values, more power is allocated over the direct link, since the path loss is lower. However, since the threshold of the direct link is also lower, as the SNR increases, more power is allocated over the dual-hop link. It can be noted that, after the value $P_{s,\max}/(WN_0) = 16$ dB, although there is more power available at the source for transmission ($P_{s,\max}$), this is not actually transmitted since both CCs have reached the thresholds set by the PUs.

Similar observations can be made for DF relaying as in the AF relaying case, but some differences are also very important to note. First, the power allocated over the dual-hop links does

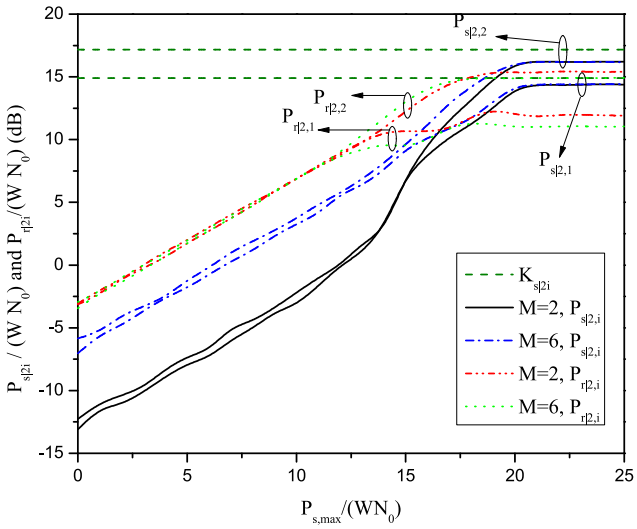

Fig. 7. Power allocation at the source and the relay over the high-frequency band, when DF relaying is applied, for $M = 2, 6$ available relays and for two CCs per frequency band.

not reach the threshold set by the PUs, despite the fact that the direct links reach the corresponding thresholds. This can be explained because the dual-hop link is now constrained by the total capacity of either the first or the second hop. This means that either the power of the source or the power of the relay will reach the threshold, so on average, the power transmitted over the second band is lower than the power allowed by the PUs. Another important feature is that the power allocated over the second band is higher, compared to the AF case, for low SNR values. This can be interpreted by the ability of the DF protocol to denoise the information that is received at the relay and redistribute it over the available CCs, which improves the performance in the low SNR region. Thus, the dual-hop link contributes more to the improvement of the achievable rate and it is preferred during the power optimization.

Figs. 6 and 7 depict the power allocation over the low- and the high-frequency band, respectively, for DF relaying with two

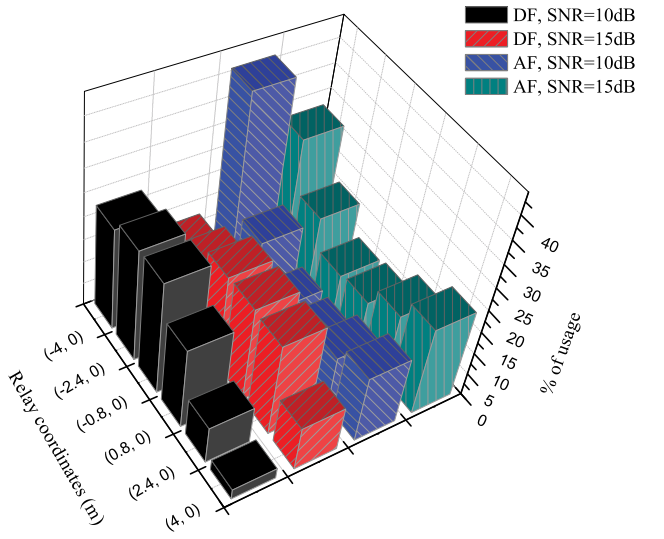

Fig. 8. Relay usage (%) for AF and DF relaying, when one CC per band and $M = 6$ relays are available, for SNR=10,15 dB.

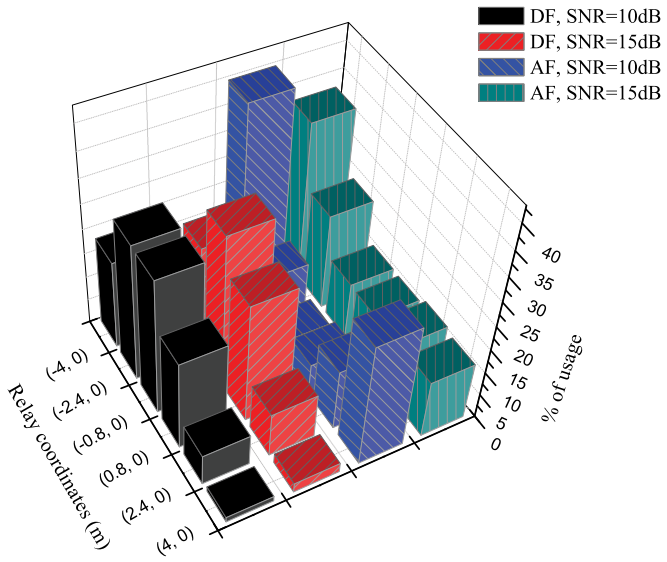

Fig. 9. Relay usage (%) for AF and DF relaying, when two CCs per band and $M = 6$ relays are available, for SNR=10,15 dB.

CCs per band, and for two different values of available relays, i.e., $M = 2, 6$. Inspecting Fig. 6, it can be easily observed that the power, which is allocated over the two CCs of the low-frequency band decreases, as the number of available relays increases. This is due to the availability of more paths for the dual-hop high-frequency link, which is preferred by the power allocation optimization. It can be noted, however, that for both cases of available relays, during the second time slot, the power transmitted by the source is allocated in the same way over the two frequencies of the direct link, since it is not affected by the dual-hop link configuration. Finally, $P_{s|1,2}$ is always higher than $P_{s|1,1}$, because the corresponding PU is situated farther, and thus, it sets a higher power threshold.

Fig. 7 depicts the power allocation over the high-frequency band, for both the source and the selected relay. Regarding the power allocation at the source, it is evident that, when the number of available relays increases, more power is allocated over both available CCs, because the dual-hop links are preferred over the direct links. Moreover, similarly to the direct links, $P_{s|2,2}$ is always higher than $P_{s|2,1}$, since the corresponding PU is situated at a greater distance and the power threshold is greater. Again, as it was observed in the case of one CC per band, the power allocated over both CCs does not reach, on average, the threshold set by the PUs. Finally, we observe that the power allocation at the selected relay is similar for both cases of available relays. The value of $P_{r|2,2}$ seems to be increasing with the number of available relays for this specific node configuration, but this depends on the positioning of the nodes, and the percentage of usage regarding each of the available relays.

Finally, Figs. 8 and 9 present the percentage of usage of each relay, when $M = 6$ relays are available, for SNR= 10,15 dB, when one or two CCs per band are aggregated, respectively. These figures offer intuitive conclusions on the relay selection, for different cases of available power, different protocols and different number of aggregated CCs. In Fig. 8, the black and red columns correspond to the DF relaying protocol, for SNR= 10 dB and SNR= 15 dB, respectively. One can observe that, when less transmit power is available, the relays closer to the SU source are preferred, while as the available power increases, the relays in the middle of the distances are preferred. This is expected, due to the following reason: In this scenario, it was considered that the selected relay transmits with the same total power as the source. However, only a portion of the source transmit power is allocated over the dual-hop link. Therefore, the first hop is weaker, and the relay selection tends to "shorten" the first hop, in order to avoid a bottleneck. However, as the power increases, the thresholds of the PUs become more important and none of the two hops becomes a bottleneck due to the transmitted power, so the selection tends to split the total distance in the middle. However, the percentages of all relays do not differ much, because the DF protocol denoises the signal. This, however, is not the case with AF relaying (blue and green columns). In this case, for both SNR values, it is observed that the relay closest to the source is most frequently selected. In that case, the noise amplification of the AF protocol is lower. Furthermore, especially for low SNR, the relay selection tends to prefer either the first or the sixth relay, because they are situated at the greatest distance from the PUs. This is not so evident for high SNR values, since—again—all the relays' transmit power values are comparable to the thresholds set by the PUs.

In Fig. 9, the same metrics as in Fig. 8 are presented, when two CCs per band are available. The conclusions are similar as in the case of one CC per band, but one difference can be observed. In the case of DF relaying, the percentages of all relays are not comparable, and the tendencies to select, either the relays closest to the source, when SNR=10 dB, or the relays in the middle, when SNR=15 dB, are now more prominent. This can be explained by the fact that the advantages of both CCs of the dual-hop link are similar, since they depend on the positioning of the node, so the preferences of the relay selection over the available relays are now more evident. A similar tendency can be observed for the AF protocol as well, that is, the preference of the first relay is more prominent when two CCs per band are available.

IX. Conclusion

In this paper, we formulated the problem of joint relay selection and optimal power allocation in underlay CR networks with CA. In the provided analysis, we considered multiple CCs, both DF and AF relaying protocols, average interference thresholds that are set by the PUs, and feedback quantization. The corresponding optimization problems have been optimally solved, using solely convex optimization, i.e., dual decomposition and an efficient iterative method. Thus, all provided solutions can be calculated in polynomial time, which is suitable for the practical implementation of the proposed scheme. Please note that the derived results can be directly extended to more frequency bands, as long as one selected relay is assumed and the frequency bands utilized by the relay are different than the ones assigned to the direct link.

Extensive simulation results were presented, which provided the following interesting conclusions. First, it was verified that the application of CA in cognitive networks, with proper joint power allocation and relay selection, can exploit the available bandwidth and boost the rate that the SU achieves, while the PUs still enjoy the desired QoS. Second, the results illustrated an interesting tradeoff between the SU's performance and the number of quantization bits for the PUs' feedback; it was shown that only a few quantization bits can offer approximately the same performance gain to the SU network as in the case of full PU feedback. Finally, it was observed that the allocated power over each CC and the percentage of usage of each relay depend both on the positioning of the nodes and on the relaying protocol, which is used, highlighting the importance of the selection of the best-situated relay and the corresponding allocation of the available transmit power.

Appendix A
Proof of Theorem 1

The Lagrangian for the *primal problem* (27) is given by

$$\begin{aligned}\Lambda(\mathcal{P}_s,\mathcal{P}_r,\lambda_1,\lambda_2,\lambda_3,\lambda_4)&=\sum_{i=1}^{N_1}\frac{1}{2}W_{1,i}\log_2(1+\gamma_{1,i})+R\\&-\lambda_1\left(\sum_{l=1}^{2}\sum_{i=1}^{N_l}P_{s|l,i}-P_{s,\max}\right)\\&-\lambda_2\left(\sum_{i=1}^{N_2}P_{r|2,i}-P_{r,\max}\right)\\&+\lambda_3\left(\sum_{i=1}^{N_2}\frac{1}{2}W_{2,i}\log_2(1+\gamma_{sr|2,i})-R\right)\\&+\lambda_4\left(\sum_{i=1}^{N_2}\frac{1}{2}W_{2,i}\log_2(1+\gamma_{sr|2,i})-R\right)\end{aligned}\tag{51}$$

where $\lambda_1,\lambda_2,\lambda_3,\lambda_4>=0$ are the LMs corresponding to the constraints $C4, C6, C7$, and $C8$, respectively. The constraints $C1$ and $C3$ will be absorbed into the KKT conditions. The *dual problem* is given by

$$\min_{\lambda_1,\lambda_2,\lambda_3,\lambda_4}\ \max_{\mathcal{P}_s,\mathcal{P}_r}\Lambda(\mathcal{P}_s,\mathcal{P}_r,\lambda_1,\lambda_2,\lambda_3,\lambda_4).\tag{52}$$

From the KKT conditions, it must hold that

$$\frac{\partial\Lambda(\mathcal{P}_s,\mathcal{P}_r,\lambda_1,\lambda_2,\lambda_3,\lambda_4)}{\partial R}=0.\tag{53}$$

By solving the aforementioned, the following equation is extracted:

$$\lambda_4=1-\lambda_3.\tag{54}$$

Thus, the Lagrangian is simplified to

$$\begin{aligned}\tilde{\Lambda}(\mathcal{P}_s,\mathcal{P}_r,\lambda_1,\lambda_2,\lambda_3)&=\sum_{i=1}^{N_1}\frac{1}{2}W_{1,i}\log_2(1+\gamma_{1,i})\\&+\frac{1}{2}\sum_{i=1}^{N_2}W_{2,i}\log_2(1+\gamma_{rd|2,i})\\&-\lambda_1\left(\sum_{l=1}^{2}\sum_{i=1}^{N_l}P_{s|l,i}-P_{s,\max}\right)\\&-\lambda_2\left(\sum_{i=1}^{N_2}P_{r|2,i}-P_{r,\max}\right)\\&+\frac{\lambda_3}{2}\left(\sum_{i=1}^{N_2}W_{2,i}\log_2(1+\gamma_{sr|2,i})\right.\\&\left.-\sum_{i=1}^{N_2}W_{2,i}\log_2(1+\gamma_{rd|2,i})\right).\end{aligned}\tag{55}$$

Therefore, the simplified dual problem is now given by

$$\min_{\lambda_1,\lambda_2,\lambda_3}\ \max_{\mathcal{P}_s,\mathcal{P}_r}\tilde{\Lambda}(\mathcal{P}_s,\mathcal{P}_r,\lambda_1,\lambda_2,\lambda_3).\tag{56}$$

According to the KKT conditions, it must hold that

$$\begin{aligned}\frac{\partial\tilde{\Lambda}(\mathcal{P}_s,\mathcal{P}_r,\lambda_1,\lambda_2)}{\partial P_{s|1,i}}&=\frac{\partial\tilde{\Lambda}(\mathcal{P}_s,\mathcal{P}_r,\lambda_1,\lambda_2)}{\partial P_{s|2,i}}\\&=\frac{\partial\tilde{\Lambda}(\mathcal{P}_s,\mathcal{P}_r,\lambda_1,\lambda_2)}{\partial P_{r|2,i}}=0\end{aligned}\tag{57}$$

which yield (28)–(30), respectively.

Appendix B
Proof of Theorem 2

The Lagrangian for the primal problem (38) is given by

$$\Lambda(\mathcal{P}_s,\lambda_1)=\frac{1}{2}\mathcal{R}_{1|r}+\mathcal{R}_{2|r}^{\mathrm{DF}}-\lambda_1\left(\sum_{l=1}^{2}\sum_{i=1}^{N_l}P_{s|l,i}-P_{s,\max}\right)\tag{58}$$

where $\lambda_1>=0$ is the LM corresponding to the constraint C_4. The constraint $\tilde{\mathrm{C}}1$ will be absorbed into the KKT conditions. The dual problem can be written as $\min_{\lambda_1}\ \max_{\mathcal{P}_s}\Lambda(\mathcal{P}_s,\lambda_1)$.

The dual problem can be solved iteratively, where in each iteration in Layer 1, the subproblems of the power allocation of the source are solved for the corresponding fixed set of LMs, which are updated in Layer 2. Please note that only one subproblem is now solved for the second band in each iteration. Applying the KKT conditions, it holds that

$$\frac{\partial\Lambda(\mathcal{P}_s,\lambda_1)}{\partial P_{s|1,i}}=\frac{\partial\Lambda(\mathcal{P}_s,\lambda_1)}{\partial P_{s|2,1}}=0\tag{59}$$

and after some manipulations (39) is derived.

APPENDIX C
PROOF OF THEOREM 3

The Lagrangian for the primal problem (42) is given by

$$\Lambda(\mathcal{P}_s,\mathcal{P}_r,\lambda_1,\lambda_2)=\frac{1}{2}\mathcal{R}_{1|r}+\tilde{\mathcal{R}}_{2|r}^{\mathrm{AF}} - \lambda_1\left(\sum_{l=1}^{2}\sum_{i=1}^{N_l}P_{s|l,i}-P_{s,\max}\right) - \lambda_2\left(\sum_{i=1}^{N_2}P_{r|2,i}-P_{r,\max}\right) \tag{60}$$

where $\lambda_1,\lambda_2>=0$ are the LMs corresponding to the constraints C_4 and C_6. The constraints C_1 and C_3 will be absorbed into the KKT conditions. The dual problem is given by

$$\min_{\lambda_1,\lambda_2}\ \max_{\mathcal{P}_s,\mathcal{P}_r}\Lambda(\mathcal{P}_s,\mathcal{P}_r,\lambda_1,\lambda_2). \tag{61}$$

Applying the KKT conditions, (39) and (45) are derived.

APPENDIX D
PROOF OF THEOREM 4

The Lagrangian for the primal problem (49) is given by

$$\Lambda(\mathcal{P}_s,\lambda_1)=\frac{1}{2}\mathcal{R}_{1|r}+\mathcal{R}_{2|r}^{\mathrm{AF}}-\lambda_1\left(\sum_{l=1}^{2}\sum_{i=1}^{N_l}P_{s|l,i}-P_{s,\max}\right) \tag{62}$$

where $\lambda_1\geq 0$ is the LM that corresponds to the constraint C_4. The constraint $\tilde{\mathrm{C}}_1$ will be absorbed into the KKT conditions. The dual problem can be written as $\min_{\lambda_1}\ \max_{\mathcal{P}_s}\Lambda(\mathcal{P}_s,\lambda_1)$. Applying the KKT conditions, (50) is derived.

REFERENCES

[1] A. Goldsmith, S. A. Jafar, I. Maric, and S. Srinivasa, "Breaking spectrum gridlock with cognitive radios: An information theoretic perspective," *Proc. IEEE*, vol. 97, no. 5, pp. 894–914, May 2009.

[2] V. N. Q. Bao, T. Duong, A. Nallanathan, and C. Tellambura, "Effect of imperfect channel state information on the performance of cognitive multihop relay networks," in *Proc. IEEE Global Commun. Conf.*, Dec. 2013, pp. 3458–3463.

[3] M. Seyfi, S. Muhaidat, and J. Liang, "Relay selection in cognitive radio networks with interference constraints," *IET Commun.*, vol. 7, no. 10, pp. 922–930, Jul. 2013.

[4] Y. Liu, Z. Ding, M. Elkashlan, and J. Yuan, "Non-orthogonal multiple access in large-scale underlay cognitive radio networks," *IEEE Trans. Veh. Technol.*, vol. 65, no. 12, pp. 10152–10157, Dec. 2016.

[5] S. Gezici, H. Celebi, H. V. Poor, and H. Arslan, "Fundamental limits on time delay estimation in dispersed spectrum cognitive radio systems," *IEEE Trans. Wireless Commun.*, vol. 8, no. 1, pp. 78–83, Jan. 2009.

[6] S. Buljore *et al.*, "Architecture and enablers for optimized radio resource usage in heterogeneous wireless access networks: The IEEE 1900.4 Working Group," *IEEE Commun. Mag.*, vol. 47, no. 1, pp. 122–129, Jan. 2009.

[7] J. D. Poston and W. D. Horne, "Discontiguous OFDM considerations for dynamic spectrum access in idle TV channels," in *Proc. IEEE 1st Int. Symp. New Frontiers Dyn. Spectr. Access Netw.*, Nov. 2005, pp. 607–610.

[8] R. Rajbanshi, A. M. Wyglinski, and G. J. Minden, "An efficient implementation of NC-OFDM transceivers for cognitive radios," in *Proc. 1st Int. Conf. Cogn. Radio Oriented Wireless Netwo. Commun.*, Jun. 2006, pp. 1–5.

[9] D. Chen, Q. Zhang, and W. Jia, "Aggregation aware spectrum assignment in cognitive Ad-hoc networks," in *Proc. 3rd Int. Conf. Cogn. Radio Oriented Wirel. Networks Commun.*, May 2008, pp. 1–6.

[10] J. Jia, Q. Zhang, and X. Shen, "HC-MAC: A hardware-constrained cognitive MAC for efficient spectrum management," *IEEE J. Sel. Areas Commun.*, vol. 26, no. 1, pp. 106–117, Jan. 2008.

[11] M. Iwamura, K. Etemad, M.-H. Fong, R. Nory, and R. Love, "Carrier aggregation framework in 3GPP LTE-advanced [WiMAX/LTE Update]," *IEEE Commun. Mag.*, vol. 48, no. 8, pp. 60–67, Aug. 2010.

[12] Z. Shen, A. Papasakellariou, J. Montojo, D. Gerstenberger, and F. Xu, "Overview of 3GPP LTE-advanced carrier aggregation for 4G wireless communications," *IEEE Commun. Mag.*, vol. 50, no. 2, pp. 122–130, Feb. 2012.

[13] C. S. Park, L. Sundstrom, A. Wallen, and A. Khayrallah, "Carrier aggregation for LTE-advanced: Design challenges of terminals," *IEEE Commun. Mag.*, vol. 51, no. 12, pp. 76–84, Dec. 2013.

[14] Q. Zhang, J. Jia, and J. Zhang, "Cooperative relay to improve diversity in cognitive radio networks," *IEEE Commun. Mag.*, vol. 47, no. 2, pp. 111–117, Feb. 2009.

[15] J. Jia, J. Zhang, and Q. Zhang, "Relay-Assisted routing in cognitive radio networks," in *Proc. IEEE Int. Conf. Commun.*, Jun. 2009, pp. 1–5.

[16] L. Lu, Y. Li, and G. Wu, "Optimal power allocation for CR networks with direct and relay-aided transmissions," *IEEE Trans. Wirel. Commun.*, vol. 12, no. 4, pp. 1–11, Apr. 2013.

[17] S. Wang, M. Ge, and C. Wang, "Efficient resource allocation for cognitive radio networks with cooperative relays," *IEEE J. Sel. Areas Commun.*, vol. 31, no. 11, pp. 2432–2441, Nov. 2013.

[18] A. Zafar, M.-S. Alouini, Y. Chen, and R. M. Radaydeh, "Optimizing cooperative cognitive radio networks with opportunistic access," *J. Comput. Netw. Commun.*, vol. 2012, pp. 294581-1–294581-9, 2012.

[19] J. Mietzner, L. Lampe, and R. Schober, "Distributed transmit power allocation for multihop cognitive-radio systems," *IEEE Trans. Wireless Commun.*, vol. 8, no. 10, pp. 5187–5201, Oct. 2009.

[20] K. Ho-Van, P. C. Sofotasios, G. C. Alexandropoulos, and S. Freear, "Bit error rate of underlay decode-and-forward cognitive networks with best relay selection," *J. Commun. Netw.*, vol. 17, no. 2, pp. 162–171, Apr. 2015.

[21] P. L. Yeoh, T. Q. Duong, M. Elkashlan, M. Matthaiou, and N. Nasser, "Mitigating cross-network interference in cognitive spectrum sharing with opportunistic relaying," in *Proc. IEEE Int. Conf. Commun.*, Jun. 2014, pp. 1561–1566.

[22] J. Lee, H. Wang, J. G. Andrews, and D. Hong, "Outage probability of cognitive relay networks with interference constraints," *IEEE Trans. Wireless Commun.*, vol. 10, no. 2, pp. 390–395, Feb. 2011.

[23] L. Luo, P. Zhang, G. Zhang, and J. Qin, "Outage performance for cognitive relay networks with underlay spectrum sharing," *IEEE Commun. Lett.*, vol. 15, no. 7, pp. 710–712, Jul. 2011.

[24] V. N. Q. Bao, T. Q. Duong, D. Benevides da Costa, G. C. Alexandropoulos, and A. Nallanathan, "Cognitive amplify-and-forward relaying with best relay slection in non-identical Rayleigh fading," *IEEE Commun. Lett.*, vol. 17, no. 3, pp. 475–478, Mar. 2013.

[25] K.-T. Feng, P.-R. Li, and C. J.-H. Chu, "Novel design of optimal spectrum sharing for cognitive radio-enabled LTE-A multi-cell networks," *IEEE Trans. Mobile Comput.*, vol. 15, no. 10, pp. 2507–2521, Oct. 2016.

[26] F. Liu, E. Bala, E. Erkip, M. C. Beluri, and R. Yang, "Small-Cell traffic balancing over licensed and unlicensed bands," *IEEE Trans. Veh. Technol.*, vol. 64, no. 12, pp. 5850–5865, Dec. 2015.

[27] Y. Fu, L. Ma, and Y. Xu, "A resource scheduling scheme for spectrum aggregation in cognitive radio based heterogeneous networks," *China Commun.*, vol. 12, no. 9, pp. 100–111, 2015.

[28] L. Fan, X. Lei, T. Q. Duong, R. Q. Hu, and M. Elkashlan, "Multiuser cognitive relay networks: Joint impact of direct and relay communications," *IEEE Trans. Wireless Commun.*, vol. 13, no. 9, pp. 5043–5055, Sep. 2014.

[29] Y. Deng, L. Wang, M. Elkashlan, K. J. Kim, and T. Q. Duong, "Generalized selection combining for cognitive relay networks over Nakagami-m fading," *IEEE Trans. Signal Process.*, vol. 63, no. 8, pp. 1993–2006, Apr. 2015.

[30] D. W. K. Ng and R. Schober, "Resource allocation and scheduling in multi-cell OFDMA systems with decode-and-forward relaying," *IEEE Trans. Wireless Commun.*, vol. 10, no. 7, pp. 2246–2258, Jul. 2011.

[31] S. B. Mohamad, C. Y. Leow, and T. A. Rahman, "Relay placement for inter-band carrier aggregation with asymmetrical coverage," in *Proc. IEEE Symp. Wireless Technol. Appl.*, Sep. 2013, pp. 108–113.

[32] L. Li, X. Zhou, H. Xu, G. Y. Li, D. Wang, and A. Soong, "Simplified relay selection and power allocation in cooperative cognitive radio systems," *IEEE Trans. Wireless Commun.*, vol. 10, no. 1, pp. 33–36, Jan. 2011.

[33] X. Liu, B. Zheng, and W. Ji, "Cooperative relay with power control in cognitive radio networks," in *Proc. 6th Int. Conf. Wireless Commun. Netw. Mobile Comput.*, Sep. 2010, pp. 1–5.

[34] X. Liu, B. Zheng, J. Cui, and W. Ji, "A new scheme for power allocation in cognitive radio networks based on cooperative relay," in *Proc. 12th IEEE Int. Conf. Commun. Technol.*, Nov. 2010, pp. 861–864.

[35] J. Lee, H. Wang, J. G. Andrews, and D. Hong, "Outage probability of cognitive relay networks with interference constraints," *IEEE Trans. Wireless Commun.*, vol. 10, no. 2, pp. 390–395, Feb. 2011.
[36] J. Si, Z. Li, and Z. Liu, "Threshold based relay selection protocol for wireless relay networks with interference," in *Proc. IEEE Int. Conf. Commun.*, May 2010, pp. 1–5.
[37] S. Boyd and L. Vandenberghe, *Convex Optimization*. Cambridge, U.K.: Cambridge Univ., 2009.
[38] S. Boyd, L. Xiao, and A. Mutapcic, "Subgradient methods," in *Lecture Notes of EE392o*. Stanford, CA, USA: Stanford Univ., Autumn Quarter 2003.
[39] M. O. Hasna and M. S. Alouini, "Performance analysis of two-hop relayed transmissions over Rayleigh fading channels," in *Proc. IEEE 56th Veh. Technol. Conf.*, vol. 4, 2002, pp. 1992–1996.
[40] P. D. Diamantoulakis, G. D. Ntouni, K. N. Pappi, G. K. Karagiannidis, and B. S. Sharif, "Throughput maximization in multicarrier wireless powered relaying networks," *IEEE Wirel. Commun. Lett.*, vol. 4, no. 4, pp. 385–388, Aug. 2015.

Panagiotis D. Diamantoulakis (S'13) was born in Thessaloniki, Greece, in 1989. He received the Diploma degree in electrical and computer engineering from the Aristotle University of Thessaloniki, Thessaloniki, in 2012, where he is currently working toward the Ph.D. degree with the Department of Electrical and Computer Engineering.

His research interests include energy and spectral efficiency, energy harvesting, wireless power transfer, cooperative systems, and smart grid.

Koralia N. Pappi (S'08–M'15) was born in Thessaloniki, Greece. She received the Diploma degree and Ph.D. degree in electrical and computer engineering from the Aristotle University of Thessaloniki, Thessaloniki, in 2010 and 2015, respectively.

In 2015, she joined Intracom S.A. Telecom Solutions, where she is part of the Ericsson Diameter Signaling Controller (Ericsson DSC) node development team. Since 2015, she has also been an adjunct Postdoctoral Researcher with the Wireless Communications Systems Group, Department of Electrical and Computer Engineering, Aristotle University of Thessaloniki. Her research interests include interference mitigation in multiuser networks, multiple access techniques, energy harvesting and wireless power transfer, resource allocation optimization, cooperative systems, cognitive networks, and modulation and diversity techniques for wireless communications. She is the coauthor of the Greek edition of a book on telecommunications systems and the coauthor of a book chapter on interference mitigation for 5G systems.

Dr. Pappi has served as a member of the Technical Program Committee of various international conferences, and she was an exemplary reviewer for IEEE TRANSACTIONS ON COMMUNICATIONS for 2015. She received the Distinction Scholarship Award of the Research Committee of the Aristotle University of Thessaloniki for the year 2012.

Sami Muhaidat (S'01–M'07–SM'11) received the Ph.D. degree in electrical and computer engineering from the University of Waterloo, Waterloo, ON, Canada, in 2006.

From 2007 to 2008, he was an NSERC Postdoctoral Fellow with the Department of Electrical and Computer Engineering, University of Toronto, Toronto, ON, Canada. From 2008 to 2012, he was an Assistant Professor with the School of Engineering Science, Simon Fraser University, Burnaby, BC, Canada. He is currently an Associate Professor with Khalifa University and a Visiting Reader with the Faculty of Engineering, University of Surrey, Guildford, U.K. He is also a Visiting Professor with the Department of Electrical and Computer Engineering, University of Western Ontario, London, ON, Canada. His research interests include advanced digital signal processing techniques for communications, cooperative communications, vehicular communications, multiple-input and multiple-output, and machine learning. He has authored more than 130 technical papers on these topics.

Dr. Sami currently serves as a Senior Editor for the IEEE COMMUNICATIONS LETTERS, an Editor for the IEEE TRANSACTIONS ON COMMUNICATIONS, and an Associate Editor for the IEEE TRANSACTIONS ON VEHICULAR TECHNOLOGY. He received several scholarships during his undergraduate and graduate studies. He was also a winner of the 2006 NSERC Postdoctoral Fellowship competition.

George K. Karagiannidis (M'96–SM'03–F'14) was born in Pithagorion, Samos Island, Greece. He received the University Diploma and Ph.D. degrees in electrical and computer engineering from the University of Patras, Patras, Greece, in 1987 and 1999, respectively.

From 2000 to 2004, he was a Senior Researcher with the Institute for Space Applications and Remote Sensing, National Observatory of Athens, Athens, Greece. In June 2004, he joined the faculty of the Aristotle University of Thessaloniki, Thessaloniki, Greece, where he is currently a Professor with the Electrical and Computer Engineering Department and the Director of Digital Telecommunications Systems and Networks Laboratory. He is also Honorary Professor with South West Jiaotong University, Chengdu, China. His research interests include the broad area of digital communications systems and signal processing, with emphasis on wireless communications, optical wireless communications, wireless power transfer and applications, molecular communications, communications and robotics, and wireless security. He is the author or coauthor of more than 400 technical papers published in scientific journals and presented at international conferences. He is also an author of the Greek edition of a book on telecommunications systems and coauthor of the book *Advanced Optical Wireless Communications Systems* (Cambridge University, 2012).

Dr. Karagiannidis has been involved as the General Chair, the Technical Program Chair, and a member of Technical Program Committees in several IEEE and non-IEEE conferences. In the past, he was an Editor for THE IEEE TRANSACTIONS ON COMMUNICATIONS, a Senior Editor of IEEE COMMUNICATIONS LETTERS, an Editor of the *EURASIP Journal of Wireless Communications & Networks* and several times a Guest Editor for the IEEE SELECTED AREAS IN COMMUNICATIONS. From 2012 to 2015, he was the Editor-in Chief of the IEEE COMMUNICATIONS LETTERS. He is one of the highly cited authors across all areas of electrical engineering, recognized as 2015 and 2016 Thomson Reuters highly cited researcher.

Tamer Khattab (M'94) received the B.Sc. and M.Sc. degrees in electronics and communications engineering from Cairo University, Giza, Egypt, in 1993 and 2000, respectively, and the Ph.D. degree in electrical and computer engineering from the University of British Columbia, Vancouver, Canada, in 2007.

He joined Qatar University (QU), Doha, Qatar, in 2007, where he is currently an Associate Professor of electrical engineering. He is also a Senior Member of the Technical Staff with Qatar Mobility Innovation Center, an R&D center owned by QU and funded by Qatar Science and Technology Park. Between 2006 and 2007, he was a Postdoctoral Fellow with the University of British Columbia working on prototyping advanced Gigabit/s wireless LAN baseband transceivers. During 2000–2003, he joined Alcatel Canadas Network and Service Management R&D, Vancouver, BC, Canada, as a Member of the Technical Staff working on the development of core components for Alcatel 5620 network and service manager. Between 1994 and 1999, he was with IBM wtc. Egypt as a Software Development Team Lead working on development of several client-server corporate tools for IBM labs. His research interests include physical layer transmission techniques in optical and wireless networks, information theoretic aspects of communication systems, and MAC layer protocol design and analysis.